Hydration of the Dienic Lipid Dioctadecadienoylphosphatidylcholine in the Lamellar Phase—An Infrared Linear Dichroism and X-Ray Study on Headgroup Orientation, Water Ordering, and Bilayer Dimensions

H. Binder,* T. Gutberlet,* A. Anikin,# and G. Klose*

*Universität Leipzig, Institut für Experimentelle Physik I, D-4103 Leipzig, Germany, and #Lomonossow State Academy of Fine Chemical Technology, Moscow, Russia

ABSTRACT In the phospholipid 1,2-*bis*(2,4-octadecadienoyl)-*sn*-glycero-3-phosphorylcholine (DODPC) in each of the fatty acid chains, a rigid diene group is inserted in a position near the polar/apolar boundary that is exceptionally sensitive for membrane stability. DODPC transforms upon gradual dehydration from the liquid-crystalline to a metastable gel state, which rearranges into two subgel phases at low and intermediate degrees of hydration. The molecular dimensions of the respective bilayers were determined by means of x-ray diffraction. Infrared linear dichroism of selected vibrations of the phosphate and trimethylammonium groups and of the ν_{13}(OH) band of water adsorbed onto the lipid was used to study the molecular order in the polar part of the bilayers in macroscopically oriented samples. The dense packing of the tilted acyl chains in the subgel causes the in-plane orientation of the phosphatidylcholine headgroups with direct interactions between the phosphate and trimethylammonium groups, and a strong orientation of adsorbed water molecules. In the more disordered gel, the thickness of the polar part of the bilayer increases and the lateral interactions between the lipid headgroups weaken. The higher order in the headgroup region of the subgels correlates with shorter decay lengths of the repulsive forces acting between opposite membrane surfaces. This result can be understood if the work to dehydrate the lipid is determined to a certain degree by the work to break up the lipid-water interactions without compensation by adequate lipid-lipid contacts. Almost similar area compressibility moduli are found in the liquid-crystalline and solid phases. Obviously, the lipid avoids lateral stress by the structural rearrangement.

INTRODUCTION

Studies of how lipid structure and thermodynamic properties vary as the lipid is varied are important tools for improving our basic knowledge about membrane stability and function (Sun et al., 1996; O'Leary and Mason, 1996). Several strategies can be applied to alter the balance of interactions within the bilayer. One approach is implicated by the amphiphilic character of the lipid molecule and suggests varying the number of methylene segments or the degree of unsaturation of the hydrocarbon chains on the one hand (Sun et al., 1996; Snyder et al., 1996; Koenig et al., 1997) or the character of the lipid headgroup (e.g., phosphatidylcholine or phosphatidylethanolamine, PC or PE, respectively) on the other. The recent discovery of new gel phases of hydrated long-chain PCs (Sun et al., 1996; Snyder et al., 1996) reveals limitations in the understanding of even simple lipid systems. The newly observed hydration-dependent polymorphism of diphytanoyl PC emphasizes the importance of molecular packing in the headgroup region in modulating membrane structure (Hsieh et al., 1997). A second approach comes from the idea of modifying the lipids at a position near the polar/apolar interface that is known to be exceptionally sensitive for membrane stability because of its pivotal location (Lewis et al., 1996). Subtle chemical modifications in this region have the potential to affect the structure and phase behavior of lipid aggregates to an extraordinary extent. For example, one can modify the linkage between the polar and apolar parts of the lipid molecule by using ester- and ether-linked hydrocarbons (Ruocco et al., 1985; Kim et al., 1987; Lewis et al., 1996) or 1,3- and 1,2-linked analogs (Dluhy et al., 1985).

In the dienic phospholipid 1,2-*bis*(2, 4-octadecadienoyl)-*sn*-glycero-3-phosphorylcholine (DODPC) in each of the fatty acid chains, a rigid 1,4-disubstituted *trans-trans*-butadiene (diene) group is inserted between the methylene chains and the ester groups, i.e., just in a position near the polar/apolar boundary. Although dienic PCs have been investigated intensively to stabilize bilayer structures by means of polymerization (Hupfer et al., 1983; Blume, 1991, and references cited therein; Ohno et al., 1987), little is known about the details of membrane architecture on a molecular level. Many studies have been done on the preparation and analysis of polymerized liposomes that can be used as drug delivery systems (Juliano and Layton, 1980). Another application would be the preparation of biocompatible lipid-water interfaces (Lee et al., 1995). Whatever the biological significance of lipid phases, there is a considerable scientific and technical interest in these materials. Their potential utility depends at least in part on the prospects for the variability of structures that they form in dependence on external conditions. In this context, the relative humidity of the surrounding atmosphere represents

Received for publication 11 August 1997 and in final form 24 December 1997.

Address reprint requests to Dr. H. Binder, Universität Leipzig, Institut für Experimentelle Physik I, Linnèstrasse 5, D-4103 Leipzig, Germany. Tel.: +49-341-9732476; Fax: +49-341-9732479; E-mail: binder@rz.uni-leipzig.de.

0006-3495/98/04/1908/16 $2.00

an alternative variable (to, e.g., temperature) to modify the physicochemical properties of membranes of lipid monomers that attract interest as precursors of the polymerization reaction.

Our recent study was addressed to the lyotropic phase behavior of DODPC (Binder et al., 1997). To enhance our understanding of water-specific effects on headgroup/acyl chain relationships, we modified the polar interface in a definite way and investigated lipid's dependence on the degree of hydration, using hydration/dehydration equipment that allows the continuous variation of the relative humidity (RH) in a wide range. Upon scans of decreasing RH, the lipid undergoes the chain-freezing transition from the liquid-crystalline phase to a metastable gel state. After storage of the sample at low RH, the gel transforms to a crystalline subgel (designated as SG_I). Subsequent adsorption of about one water molecule per lipid induces the conversion to a second subgel (SG_{II}) at intermediate RH values. Whereas the chain melting properties of DODPC closely resemble those of 1,2-dimyristoyl-*sn*-glycero-3-phosphorylcholine (DMPC), the disaturated PC with the identical number of methylene units per acyl chain, a quite different phase behavior of both lipids was found in the rigid state. Apparent differences were attributed to the influence of the diene groups that promote the formation of crystalline subgel phases. The subgels are characterized by a denser packing of the octadecadienoyl chains within the hydrophobic core of the bilayer in comparison with the gel.

Although detailed information about acyl chain packing modes, water-lipid interactions, and conformational changes in the different parts of the lipid were obtained by means of infrared spectroscopy (Binder et al., 1997), the answer to the original question about the correlation between the molecular structure of DODPC and the architecture of the membrane build from it remains unanswered. In the present paper we studied the bilayer dimensions by means of x-ray scattering. With decreasing RH, the lipid/water multilayer stacks are exposed to an increasing osmotic pressure due to the removal of water, leading to their gradual compression (Rand, 1981; Rand and Parsegian, 1989). The changes in the bilayer dimensions were analyzed in terms of the repulsive force acting between opposite polar surfaces and the lateral compressibility modulus of the bilayer. The x-ray investigations are combined with infrared linear dichroism measurements to obtain information about the molecular order of the phosphate and trimethylammonium groups, as well as of the adsorbed water, as a function of RH. Note that this method of investigation of lipid membranes has been established for many years, but it has scarcely been applied to the study of headgroup (Fringeli, 1977; Fringeli and Gunthard, 1981; Hübner and Mantsch, 1991) and water (Okamura et al., 1990) ordering. Our IR dichroism measurements are mainly addressed to the issue of how the properties of the polar part of the bilayer correlate with the geometry of the bilayers and with the repulsive forces acting between them.

The latter question is also stimulated by the hydration force concept that has attracted wide interest in experimental (Rand, 1981; Rand and Parsegian, 1989; Gawrisch et al., 1992; McIntosh and Simon, 1993) and theoretical work (see Leikin et al., 1993, for a review). Several factors are related to interbilayer forces: water structure (Marcelja and Radic, 1976), local dipolar moments and solvent polarization (Kornyshev and Leikin, 1989; Leikin et al., 1993), and the chemical hydration of an extended "interphase" (Cevc, 1991), but so are entropic components arising from several types of thermal motions within the membranes (Israelachvili and Wennerström, 1992). The problem is to determine distinguishing features and the relative importance of these factors (Rand and Parsegian, 1989). Usually the adsorption of water is accompanied by structural modification of the polar region of the bilayer and by increasing conformational disorder in the apolar part and vice versa. These correlations make it difficult to distinguish whether the repulsive forces are caused exclusively by the membrane surface or also by underlying motions of the lipid molecules. DODPC exists in three different rigid states obeying different properties of the headgroup region, as indicated by wavenumber shifts of absorption bands originating from vibrations of the PC headgroup (Binder et al., 1997). In a wide range of RH, two different solid states of DODPC, a subgel and the gel, can be compared directly at identical external conditions (RH and temperature) by using one sample. Thus we expect that the specification of headgroup and water structure on one hand and the determination of the repulsive forces between the solid membranes on the other can give some experimental insight into the interrelation between molecular and systems properties.

MATERIALS AND METHODS

Materials

1,2-*bis*(2,4-Octadecadienoyl)-*sn*-glycero-3-phosphorylcholine (DODPC, Scheme 1) was purchased from Nippon Oil and Fats Co. The purity was confirmed by thin-layer chromatography (TLC) (eluant: chloroform/methanol/water, 65/25/4 v/v) showing a single spot on the TLC plates. Ethanolic stock solution (5 mg/ml, spectroscopic grade ethanol) of DODPC was used for sample preparation.

Infrared dichroism investigations

Sample preparation and FTIR measurements

Samples were prepared by spreading 200 μl of the stock solution homogeneously on one side of a ZnSe-attenuated total reflection (ATR) crystal (50 $\times$ 5 mm; face angle 45°) and evaporating the solvent under a stream of nitrogen. The lipid arranges spontaneously into layers oriented preferentially parallel to the crystal surface, as indicated by strong linear dichroism of the IR-absorption bands (see below). The amount of lipid corresponds to a number of lipid bilayers (on the order of 10^3), yielding an average thickness of the lipid film of >4 μm.

The ATR crystal was mounted on a commercial horizontal Benchmark unit (Specac, Belfast, UK), which was modified to realize a definite relative humidity (RH) and temperature at the crystal surface coated with the lipid (Binder et al., 1997). This equipment allows us to adjust the RH continuously to values between 5% and 98% with an accuracy of $\sim\pm1$%.

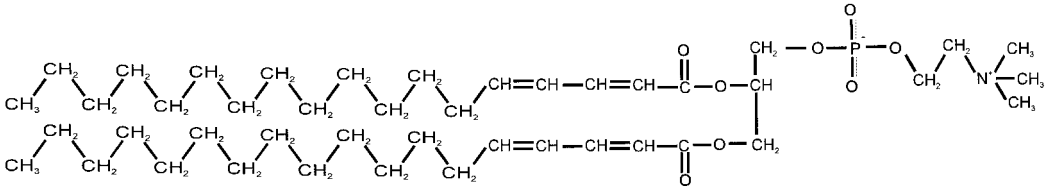

DODPC

Scheme 1

The ATR unit was placed into a BioRad FTS-60a Fourier transform infrared spectrometer (Digilab, MA) equipped with a wire grid polarizer (efficiency of >98%), which was placed between the ATR unit and the deuterated triglycine sulfate detector. Each single-channel spectrum was recorded with 128 scans at two perpendicular polarizations of the IR beam, which were adjusted by aligning the polarizer either parallel or perpendicular to the surface normal of the ATR crystal. Polarized absorbance spectra of the sample, $A_{\parallel}(\nu)$ and $A_{\perp}(\nu)$, were calculated with a resolution of 2 cm^{-1}, using the respective single-channel spectra of the empty ATR crystal as background.

The samples were investigated by means of increasing (hydration scan) as well as decreasing (dehydration scan) RH at constant temperature (T = 25 ± 0.2)°C. The RH was varied in steps of 2%. Before measurement the sample was allowed to equilibrate for 10 min after reaching the prescribed RH in each step. This period was found to be sufficient for equilibration of the sample, as has been proved by kinetic measurements and by scans with longer equilibration times in which no significant deviations of the spectral data could be detected. Note that the average scan rate used amounts to a RH change of <5%/h.

Before the hydration scan was started, the sample was stored at RH = 40% for 7–15 h, subsequently dried, and stored for several hours at RH = 8% to transform the sample into the crystalline SG_I state. Dehydration scans were started after equilibrating the lipid at RH = 98% for 2–3 h.

Determination of the infrared order parameter

If the director of a uniaxial system points perpendicular to the ATR surface, the dichroic ratio, R, of an absorption band depends on the IR order parameter, S_{IR}, of the corresponding IR active transition moment (Hübner and Mantsch, 1991):

$$R \equiv \frac{A_{\parallel}}{A_{\perp}} = \frac{A + B \cdot S_{IR}}{1 - S_{IR}} \tag{1}$$

The polarized absorbances, $A_{\parallel}$ and $A_{\perp}$, are evaluated from the polarized IR spectra, $A_{\parallel}(\nu)$ and $A_{\perp}(\nu)$, after baseline correction and by integration over the spectral range attributed to the absorption band. The constants $A = 2$ and $B = 2.55$ correspond to a film thickness exceeding the penetration depth of the electromagnetic waves and depend on the ratio of the refractive indices of the lipid sample and of the ZnSe crystal ($n_{21} = 1.44/2.4 = 0.6$) and the angle of incidence (45°) (Harrick, 1967). S_{IR} is defined as

$$S_{IR} = \frac{1}{2}\langle 3 \cdot \cos^2\theta - 1 \rangle \tag{2}$$

where θ is the angle enclosed by unit vectors parallel to an individual transition moment and the optical axis, which points perpendicular to the crystal surface. The angular bracket denotes ensemble averaging over all absorbing transition moments in the sample. After rearrangement of Eq. 1, the IR order parameter can be calculated from the dichroic ratio by means of

$$S_{IR} = \frac{R - A}{R + B} \tag{3}$$

X-ray measurements

For x-ray investigations a lipid film was spread on glass plates (20 × 25 mm) and dried. The slides were positioned into a sealed thermostatted (25°C) chamber mounted on a conventional Philips PW3020 powder diffractometer (Philips, Eindhofen, the Netherlands). X-ray powder diffractograms were obtained with Ni-filtered Cu K_α radiation (20 mA/30 kV) by $\Theta_{x\text{-ray}}/2\ \Theta_{x\text{-ray}}$ scans. Scan rates were between 1 and 10 s, with 0.01–0.02° per step. Intensity was detected with a proportional detector system. Nitrogen of definite RH was continuously streamed through the sample chamber, using the moisture-regulating unit that was also applied to FTIR measurements. The samples were equilibrated analogously. Repeat distances corresponding to multilamellar stacks of lipid bilayers are determined with an accuracy of 0.05–0.1 nm, using Bragg peaks up to the fourth order.

If the composition of the lamellar stacks is known, the mean cross-sectional area per lipid molecule at the lipid/water interface can be estimated from the repeat distance, d, by

$$A_L = \frac{2 \cdot V}{d} \tag{4}$$

where $V = (v_L + R_{W/L} \cdot v_W)$ is the volume of one DODPC molecule, v_L = 1.3 nm^3, and the volume of the water adsorbed by it (v_w = 0.03 nm^2, molecular volume of water) provided the additivity of the molecular volumes. The number of adsorbed water molecules per lipid molecule, $R_{W/L}$, which depended on the relative humidity, was determined previously (Binder et al., 1997).

The water layer thickness between opposing bilayers, d_W, and the thickness of the bilayer, d_L, were calculated by the simple approach of nonpenetrating lipid/water layers proposed by Luzzati (1968):

$$d_w = \frac{2 \cdot R_{W/L} \cdot v_w}{A_L} \quad \text{and} \quad d_L = d - d_w \tag{5}$$

The thickness of the polar interface, d_{pol}, and that of the hydrophobic core, d_{hc}, can be estimated analogously by using

$$d_{pol} = \frac{2 \cdot v_{pol}}{A_L} \quad \text{and} \quad d_{hc} = d_L - d_{pol}, \tag{6}$$

respectively, where v_{pol} = 0.344 nm^3 denotes the volume of the polar part of the lipid molecule, including the ester groups, the glycerol backbone, and the PC headgroup (Scherer, 1989; see also Rand and Parsegian, 1989, for a review).

The electron density profile of the lipid bilayer, $\rho(z)$, was calculated by

$$\rho(z) = \sum_h \pm a_h \cdot \cos(2\pi h z/d) \quad \text{with} \quad a_h = \sqrt{I_h \cdot h} \tag{7}$$

where h is the order and I_h the maximum of the Bragg reflection, respectively (see, e.g., McIntosh and Simon, 1986, and references cited therein). The signs of a_h were chosen according to the condition that the amplitudes measured at different RH must sample along the continuous Fourier transform of $\rho(z)$. The z difference of the two scattering density maxima

that result from the electron-rich phosphate groups yield directly the mean phosphate-phosphate distance, d_{PP}.

EXPERIMENTAL RESULTS AND DISCUSSION

Bilayer dimensions

Fig. 1, *a–d*, shows the diffraction pattern of DODPC in the liquid-crystalline (L_α), gel, and subgel (SG_I and SG_{II}) states, measured for decreasing (dehydration scan; phase sequence: $L_\alpha \rightarrow$gel) and increasing (hydration scan; $SG_I \rightarrow SG_{II} \rightarrow L_\alpha$) relative humidity. In all cases, a series of up to five equally spaced Bragg peaks indicates multilamellar lipid structures. In pure lipid systems of limited hydration, the coexistence of two phases is predicted for a certain water concentration range by the Gibbs phase rule (Marsh, 1990, p. 121, and references cited therein). Phase coexistence was identified by the appearance of two sets of equally spaced Bragg peaks, which can be unambiguously attributed to the lower RH and higher RH phases, respectively (see, e.g., Fig. 1, *e* and *f*). The two-phase ranges extending to RH = 67%–55% (L_α/gel), 75%–85% (SG_{II}/L_α), and 58%–60% (SG_I/SG_{II}), respectively (see also Binder et al., 1997), are excluded from the data analysis.

Upon dehydration the repeat distance, *d*, increases distinctly in the RH range in which the lipid undergoes the L_α-gel phase transition (Fig. 2 *a*). This effect is caused mainly by the freezing of the polymethylene chains, which transform from a more disordered to an all-*trans* extended conformation. Evidence of this conformation was obtained previously by the appearance of the methylene-wagging band progression (Binder et al., 1997). The thickness of the bilayer increases by $\Delta d_L \approx 0.48$ nm, and thus corresponds to a length increment of 0.020 nm per methylene unit in each octadecadienoyl chain. The freezing of the hydrocarbon chains is accompanied by a reduction of the area per lipid, A_L, from $A_L \approx 0.55$ nm^2 to 0.50 nm^2, and by an increase in the thickness of the polar region of the bilayer, d_{pol}, from $d_{pol} \approx 0.62$ nm to 0.7 nm.

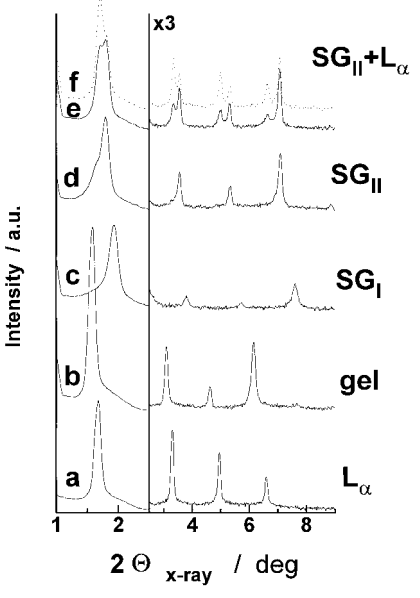

FIGURE 1 X-ray diffraction pattern of DODPC in the different phases measured at relative humidities. (*a*) 90% (L_α), (*b*) 10% (gel), (*c*) 10% (SG_I), (*d*) 60% (SG_{II}), (*e*) 80% (SG_{II} + L_α), (*f*) 85% (SG_{II} + L_α). (*a–f*) Dehydration (*a*, *b*) and hydration scans (*c-f*). The Bragg peaks of higher order are amplified by a factor of 3.

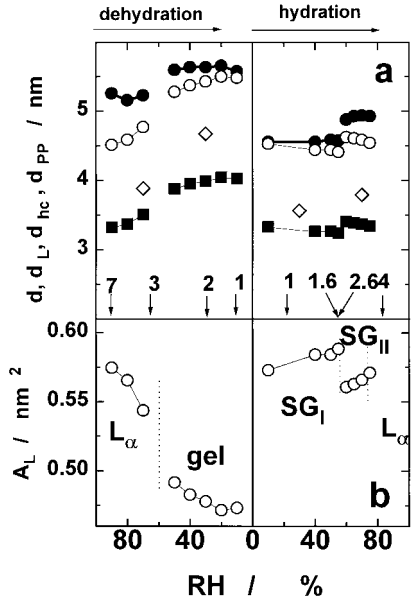

FIGURE 2 Bilayer dimensions of DODPC as a function of the relative humidity. (*a*) Repeat distances, *d* (●); thickness of the membrane, d_L (○), and of the hydrophobic core, d_{hc} (■); and the phosphate-phosphate distances, d_{PP} (◇). (*b*) The area per lipid, A_L. The phases of DODPC are indicated in *b* in the respective RH ranges. The number of adsorbed water molecules per lipid ($R_{W/L}$) is given at selected RH values at the lower coordinate axis in *a*.

After the lipid is stored at low RH for several hours (see above), it undergoes a transition from the gel to the SG_I phase, which is characterized by a drastically reduced repeat distance. This effect can be explained by an expansion of the surface and by using (in addition to Eq. 6) a reduction of both d_{pol} and d_{hc} (cf. Fig. 2, *a* and *b*). The adsorption of one additional water molecule per lipid with increasing RH at the SG_I-SG_{II} transformation reverses these tendencies slightly.

The phosphorus-phosphorus distance, d_{PP}, taken from the electron density profiles (Fig. 3), lies in the range between d_{hc} and d_L. The peaks of the electron density become relatively sharp in the SG_I and relatively wide in the gel state, and thus the widths of the maxima correlate with the estimates of the vertical extent of the polar region of the bilayer in the subgel and gel, $d_{pol} \approx 0.6$ nm and 0.7 nm, respectively. Note that d_{pol} is smaller than the headgroup thickness of 1 nm assumed by McIntosh and Simon (1986) from space-filled molecular models. We estimate that five (L_α) or seven or eight (gel, subgel) water molecules should be located "inside" the polar region to increase their thickness to 1 nm. The latter values at least are unrealistic, in

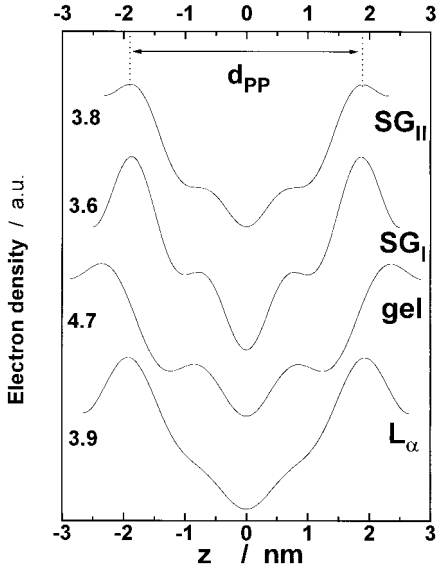

FIGURE 3 Typical electron density profiles of a bilayer in the different phases of DODPC. The intrabilayer peak-to-peak separations, d_{PP}, are given in the figure in nanometers. The z coordinate denotes the distance from the bilayer center.

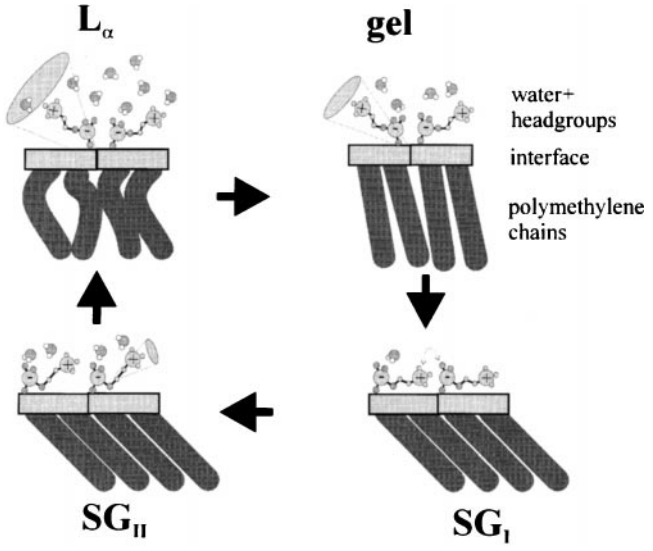

FIGURE 4 Schematic representation of the molecular arrangement of DODPC in the different phases. Only one-half of the bilayer is shown. The motional freedom of the headgroups is indicated by cones forming the boundary of reorientations. The detailed molecular packing in the region of the glycerol, ester, and diene groups is not yet clear, and therefore this region is symbolized by rectangles.

view of the small number of water molecules adsorbed onto the lipid in the rigid state ($R_{W/L} < 4$). Scherer (1989) estimated that about three to seven water molecules are located "inside" the polar region of PC lipids at full hydration.

Under all conditions the electron density profiles show the well-defined trough at the bilayer center, which is characteristic for a regular (i.e., noninterdigitated) bilayer structure (Kim et al., 1987; Ruocco et al., 1985). Thus, excluding the possibility of interdigitation, the marked changes in A_L and d_L in the subgels with respect to the gel state can be explained by the appearance of or increase in the tilting of the acyl chain axes (cf. Fig. 4 for an illustration).

The length of the CH_3-$(CH_2)_{12}$-CH═CH-CH═CH-fragment of the octadecadienoyl chain in the all-*trans* extended conformation amounts to $L_{max} = 2.16$ nm, assuming 1.67 nm for the CH_3-$(CH_2)_{12}$-fragment (Tanford, 1973) and 0.49 nm for the diene group, using bond lengths of 0.146 nm (CH-CH) and 0.135 nm (CH═CH) and a standard bond angle of 120° (Good et al., 1981). Note that L_{max} overestimates the real length of the acyl chains in the membrane, not due least to three effects: 1) librotorsional motions about C-C single bonds, 2) the bent configuration of the chains in the *sn*-2 position, and 3) tumbling motions of the whole chain. We will take these effects into account and use a scaling factor of 0.9. Then one can estimate the mean tilt angle, γ_{tilt}, included between the acyl chain axes and the bilayer normal from d_{hc}, using the relation $\cos \gamma_{tilt} = d_{hc}/(2 \times 0.9 \times L_{max})$. In the gel and subgels of DODPC, one obtains values of 20–25° and 38–41°, respectively.

The wide-angle region of the x-ray diffractograms of DODPC measured in the subgels yields a reflection at $(d_1 = 0.41 \text{ nm})^{-1}$, with a shoulder of about half-maximum intensity at $(d_2 = 0.39 \text{ nm})^{-1}$ (not shown). This pattern is typical for a orthorhombic lattice with tilted acyl chains (Tardieu et al., 1973) and thus confirms the results deduced from the low-angle scattering data. Scattering of this nature would not be expected for interdigitated, nontilted chains that give rise to sharp, symmetrical reflections (see also Ruocco et al., 1985). In the gel state the peak sharpens slightly, and its maximum shifts to $(d_1 = d_2 = 0.42 \text{ nm})^{-1}$. The cross-sectional area occupied by the acyl chains can be calculated from the short spacings by $A_{hc} = d_1 \times d_2 \times (1 - (d_1/2 \times d_2)^2)^{-0.5}$, yielding (0.188 ± 0.05) nm^2 for the subgels and (0.203 ± 0.05) nm^2 for the gel. The estimation of the tilt angles using $\cos \gamma_{tilt} = 2 \times A_{hc}/A_L$ gives rise to apparent values of ~50° (subgels) and 45° (gel).

We conclude that in the subgels, the acyl chains of DODPC are strongly tilted, realizing in this way a denser packing within the hydrophobic core of the bilayer (cf. Fig. 4). Evidence of crystalline chain packing modes in the subgels was obtained spectroscopically by splitting the methylene bending and rocking vibrations (Binder et al., 1997). The tilt of the chain axes is usually induced by the mismatch between the cross section of the lipid headgroup and that of the acyl chains in the extended all-*trans* configuration (McIntosh, 1980). In disaturated PCs this situation leads to the formation of tilted gel and subgel phases ($P_{\beta'}$, $L_{\beta'}$, and L_c) with typical tilt angles of 30°-35° at full hydration, which decrease considerably, however (<20°), if one dehydrates the lipids (Tardieu et al., 1973; Marsh, 1990, pp. 166–167, and references cited therein). In contrast to DODPC, no significant difference between the bilayer thickness and, thus, a similar chain tilt were reported by McIntosh and Simon (1993) for 1,2-dipalmitoyl-*sn*-glycero-3-phosphorylcholine (DPPC) membranes in the gel and subgel phases at reduced hydration.

The reason for the significantly enhanced tilt angles that adopt the acyl chain axes of DODPC in the subgels should be sought in the properties of the diene moieties. Obviously these rigid groups cause steric restrictions in the vicinity of the polar/apolar interface that increase the effective area requirement per molecule within the pivotal plane of the lipid layer. Upon chain freezing, DODPC first forms a metastable gel state. The strong van der Waals attractive forces acting between the all-*trans* extended chains induce lateral stress at the polar/apolar interface, where the repulsion between the PC headgroups as well as an unspecified influence of the diene groups prevent a further approach of the lipid molecules and thus an optimal packing of the acyl chains. In the subgels thermodynamic equilibrium is reached by the denser molecular packing within the hydrophobic core, accompanied by the increased tilting of the hydrocarbon chains and the lateral expansion of the bilayers. This effect is correlated with a more favorable arrangement of the diene groups, and possibly of the PC heads as well.

Note that at a low hydration level the headgroup layer of the corresponding disaturated PC, DMPC, folds into a "sawtooth" arrangement to increase the packing density of the acyl chains (Pearson and Pascher, 1979). In this case the chain axes remain almost nontilted. Interestingly, relative big tilt angles of the hydrocarbon chains (>40°) are found in crystalline double-chained sphingosines, where the linkage between the chains and the headgroups is chemically modified compared with PCs, namely by a sphingosyl residue instead of the glycerol moiety (Pascher et al., 1992).

Headgroup orientation

Information on PC headgroup orientation (and conformation) is available from a number of characteristic IR absorption bands assigned to vibrations of the phosphate and trimethylammonium groups (Table 1; see Fringeli and Gunthard, 1981, for a review). The PO stretching vibrations correspond to the free and esterified oxygens and split into a symmetrical and antisymmetrical mode each. In the $C\text{-}N^{+}\text{-}(CH_3)_3$ unit of phosphocholines, at least four basic modes of the C-N stretching vibration are reported, two symmetrical (with respect to the $N\text{-}(CH_3)_3$ fragment, with C-N in phase and in antiphase, respectively) and two antisymmetrical ones. In addition, the wavenumbers of the corresponding absorption bands depend on the conformation of the O-C-C-N fragment (*gauche* or *trans*) (Akutsu, 1981; Fringeli and Gunthard, 1981). Some controversy has appeared concerning the assignment of the band at 875 cm^{-1}, which was attributed either to the $\nu_s(C\text{-}N)_g$ mode of the *gauche* conformation (Akutsu, 1981; Fringeli and Gunthard, 1981) or to a CH_2 rocking vibration in the choline moiety, in analogy to acetylcholine (Derreumaux et al., 1989).

TABLE 1 Assignments of selected absorption bands of DODPC originating from the PC-headgroup, their position, and the direction of the corresponding transition moments*

Group vibrations	Assignment	Symbol	Position (cm^{-1})	No.	Transition moment‖
Phosphate	$PO^{-}{}_2$ antisymmetrical stretching#	ν_{as} ($PO^{-}{}_2$)	1255–1239	1	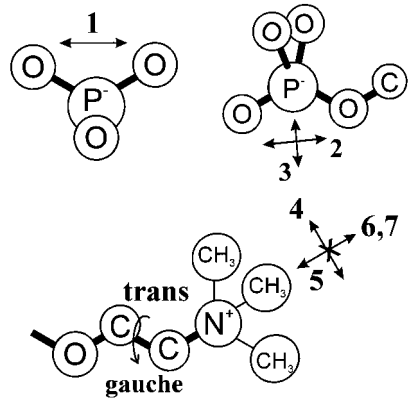
	$P\text{-}(OC)_2$ antisymmetrical stretching	$\nu_{as}(P\text{-}(OC)_2)$	826–800	2	
	$P\text{-}(OC)_2$ symmetrical stretching	$\nu_s(P\text{-}(OC)_2)$	768–763	3	
Choline (trimethylammonium)	$C\text{-}N^{+}\text{-}(CH_3)_3$ antisymmetrical stretching	$\nu_{as}(N\text{-}C)_{ip}$	970–969	4	
	$C\text{-}N^{+}\text{-}(CH_3)_3$ antisymmetrical stretching	$\nu_{as}(N\text{-}C)_{op}$	956–953	5	
	$C\text{-}N^{+}\text{-}(CH_3)_3$ symmetrical stretching§	$\nu_s(N\text{-}C)_t$	927–923	6	
	$C\text{-}N^{+}\text{-}(CH_3)_3$ symmetrical stretching¶	$\nu_s(N\text{-}C)_g$	875–873	7	
	CH_3 antisymmetrical stretching	$\nu_{as}(CH_3)_{Chol}$	3030–3021		

*The assignments and directions are taken from Fringeli and Gunthard (1981) and Akutsu (1981), and the wavenumbers are partially from Binder et al. (1997).

#The $\nu_s(PO_2)$ vibration at ~1090 cm^{-1} was not analyzed because it overlaps with a strong absorption band (1078 cm^{-1}) originating probably from a C–C mode in the conjugated C=C–C=C–C=O fragment (not shown).

§*Trans* conformation of O–C–C–N.

¶*Gauche* conformation of O–C–C–N, assignment of $\nu_s(N\text{–}C)_g$ under question, second band appears at ~900 cm^{-1}. The second mode of ν_s (N–C) (totally symmetrical) is expected at 720 cm^{-1} (*gauche*), but to be of weak intensity and overlapped by the CH_2 rocking band.

‖The arrows illustrate the direction of the transition moment of the vibration listed in column No. Isolated group frequencies are assumed (no vibrational mixing with adjacent bonds).

The directions of the transition moments of the PC-headgroup modes are given schematically in Table 1, assuming isolated group vibrations. However, this assumption fails to some degree for the P-$(OC)_2$ modes, in which C-O single bond stretching is significantly involved (Fringeli, 1977). Couplings of ν(C-N) with other vibrations also occur in the *gauche* conformation of the choline group (Fringeli and Gunthard, 1981). Despite these uncertainties, we assume that changes in the dichroism of these bands indicate variations in headgroup orientations that can be qualitatively analyzed by using the assumptions made.

The mean band positions of the PC headgroup vibrations shift markedly when DODPC transforms between the different states (Binder et al., 1997). These effects are attributed qualitatively to conformational changes of the C-O-P-O-C and O-C-C-N fragments and/or to modifications of phosphate-water and/or phosphate-trimethylammonium interactions. The polarized absorbance spectra of DODPC shown in Fig. 5 indicate that the changes in bandshape and position are accompanied by dichroic effects, suggesting PC-headgroup reorientations.

The IR order parameters of the respective transition moments are obtained by integrating the polarized spectra in the ranges shown in Fig. 5. Hence we obtained the dichroic ratio data without applying band separation by means of curve fitting. This approach is justified because the precision of the analysis in terms of headgroup orientation is limited by the model assumptions concerning the directions of the transition moments and not by uncertainties of data analysis. Note that S_{IR} is determined by the orientation of the respective transition moment with respect to the membrane normal and by the degree of macroscopic alignment of the multilamellar stacks on the ATR surface. Curved membrane areas and packing defects are expected to diminish the absolute value of S_{IR}. Consequently, the apparent inclination angle of the transition moment with respect to the membrane normal, θ (cf. Eq. 2 and *right scale* in Figs. 6 and 7), is expected to underestimate θ for $S_{IR} < 0$ and to overestimate θ for $S_{IR} > 0$.

The IR order parameters of all headgroup vibrations investigated vary with RH and show marked jumps upon transformation in the subgel phases. The S_{IR} of the C-N^+-$(CH_3)_3$ modes also changes markedly at the SG_I–SG_{II} transition, in contrast to the order parameter of the phosphate bands (cf. Figs. 6 and 7). This parallel behavior of all modes of the ammonium group on the one hand and that of the phosphate group on the other hand can be interpreted as an indication of correct band assignments.

Interpreting the IR order parameters shown in Fig. 6 in terms of the apparent inclination angle, θ, one obtains the following picture for the average phosphate group orientation (see Figs. 4 and 8 for illustrations). In the L_α phase the connecting axis of the ester oxygens includes an apparent angle of $\theta \approx 45°$ with the director. The line connecting the two nonesterified oxygens is directed preferentially parallel to the bilayer surface. Consequently, the plane made by CO-P-OC cuts the membrane surface nearly perpendicularly on the average. Upon dehydration (gel state) the CO-P-OC axis reorients slightly toward the membrane plane. At the gel-SG_I transformation, this tendency is drastically strengthened. The drop in $S_{IR}(\nu_{as}$P-$(CO)_2))$ and the rising $S_{IR}(\nu_s$P-$(CO)_2))$ indicate that the CO-P-OC axis aligns almost parallel to the membrane surface. Note that both nonesterified oxygens seem to point upward, as before,

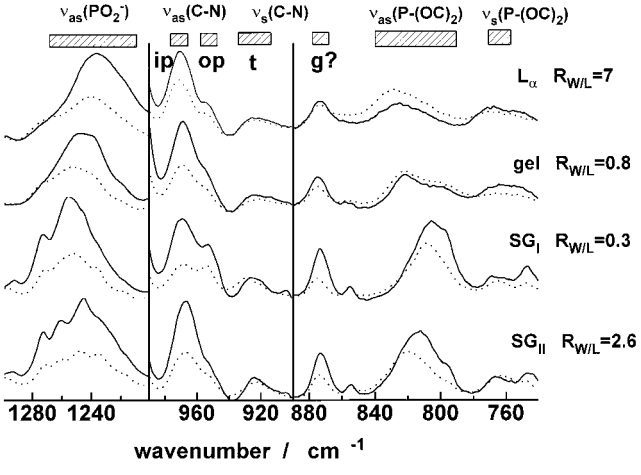

FIGURE 5 Polarized absorbance spectra, $A_{\|}(\nu)$ (·····), and $2 \times A_{\perp}(\nu)$ (——), of selected PC-headgroup vibrations of DODPC in different phases, which are indicated on the right together with the respective number of adsorbed water molecules per lipid ($R_{W/L}$). Note that the weighting factor of $A_{\perp}(\nu)$ allows direct comparison between $2 \times A_{\perp}(\nu)$ and $A_{\|}(\nu)$, which are equal for $S_{IR} = 0$ (cf. Eqs. 1 and 3). The band assignments are given at the top of the figure, together with the wavenumber ranges of integration for determination of S_{IR} (▨; see text). Absorbance units are arbitrary.

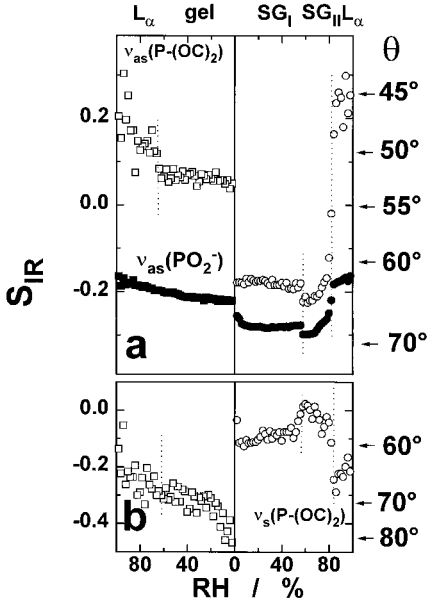

FIGURE 6 Infrared order parameter (S_{IR}) of phosphate group vibrations as a function of relative humidity. (*a*) ν_{as}P-$(OC)_2$) and $\nu_{as}(PO_2^-)$. (*b*) ν_sP-$(OC)_2$). The phases are indicated at the top, and the apparent inclination angles, θ, (cf. Equation 2) are at the right axis.

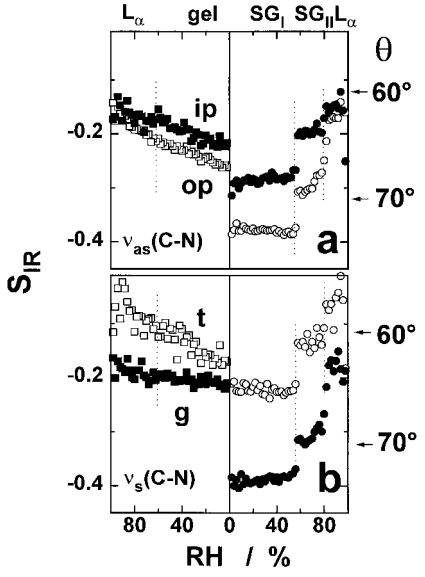

FIGURE 7 Infrared order parameter (S_{IR}) of C-N vibrations of the trimethylammonium group as a function of relative humidity. (*a*) In-plane and out-of plane mode of ν_{as}(C-N). (*b*) ν_s(C-N) assigned to *gauche* and *trans* conformations of the O-C-C-N fragment (see text). The phases are indicated at the top, and the apparent inclination angles, θ (cf. Eq. 2), are at the right axis.

because the mean orientation of the $\nu_{as}(PO_2^-)$ transition moment is virtually unchanged. The slight decrease in $S_{IR}(\nu_{as}(PO_2^-))$ probably indicates the reduction of reorientations around the CO-P-OC axis.

A similar analysis of the C-N$^+$-(CH$_3$)$_3$ modes gives rise to the following results (Figs. 7 and 8 for illustrations). The C-N bond is only slightly inclined from the bilayer surface ($\theta > 60°$), as indicated by the negative S_{IR} values of all

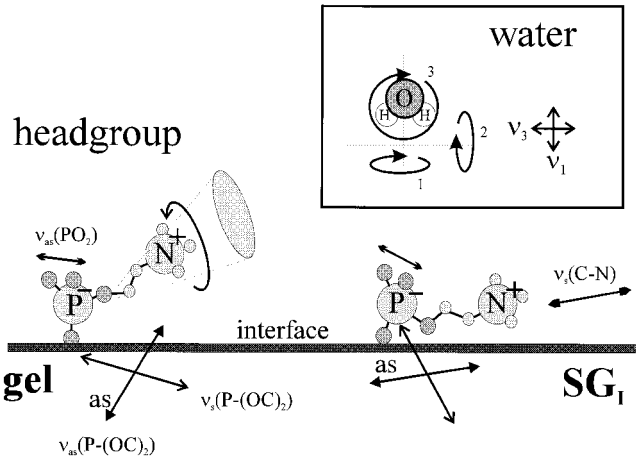

FIGURE 8 Schematic illustration of the headgroup orientation of DODPC in the gel and SG_I phases. The orientations of selected IR active transition moments corresponding to headgroup vibrations are shown by double arrows (see Table 1 for assignments). The inset gives the directions of the transition moments of the ν_1 and ν_3 modes in the isolated water molecule, and defines the principal axes 1, 2, and 3. See text for explanations.

modes obtained in the whole RH range. The decrease in the S_{IR} upon dehydration (gel) and its drop at the gel-SG_I transformation can be attributed to the increased tendency of the C-N bond to align parallel to the membrane surface and to the reduced mobility of the choline moiety at low hydration, in accordance with the behavior of the CO-P-OC axis. At the SG_I-SG_{II} transition, the negative S_{IR} of all C-N$^+$-(CH$_3$)$_3$ modes increases markedly, in contrast to the order parameters of the phosphate group. Hence this transition seems to affect the mean orientation and mobility of the terminal trimethylammonium group, whereas the rigid packing of the phosphate moiety is maintained. The almost similar behavior of the S_{IR} of the in-plane and out-of plane ν_{as}(C-N) bands in the L$_\alpha$ and gel states can be explained by nearly free rotations about the C-N bond (Fig. 7 *a*). The increased difference between the two order parameters in the subgels possibly indicates that this type of motion is reduced to a high degree, leading to an almost fixed orientation of the trimethylammonium group. The relation between the S_{IR} values of the absorption bands that are attributed to the *gauche* and *trans* conformations, $S_{IR}(\nu_s(C\text{-}N)_g) < S_{IR}(\nu_s(C\text{-}N)_t$ (Fig. 7 *b*), becomes plausible if one imagines that the *gauche* conformation of the O-C-C-N fragment inclines the terminal C-N bond toward the membrane plane. Taking into consideration that the band at $\sim$875 cm^{-1} may alternatively originate from the methylene rocking modes of the choline moiety (Derreumaux et al., 1989), the small S_{IR} values would indicate an almost perpendicular orientation of the O-C-C and the C-C-N planes with respect to the bilayer surface, because the corresponding transition moment points along the line connecting the methylene hydrogens.

This alternative interpretation, as well as the uncertainties concerning the directions of some of the transition moments, would not alter the basic conclusions about the headgroup orientation derived from the dichroism of phosphate and trimethylammonium vibrations. In general, the dichroic data are in qualitative agreement with the widely accepted concept of PC headgroup properties (see Cevc and Marsh, 1987, and references cited therein). In particular, the phosphocholine group orients nearly parallel to the membrane surface, making a small angle of the P$^-$-N$^+$ dipole with it (17°-27° for DMPC dihydrate; Pearson and Pascher, 1979). The free phosphate oxygens point upward at an angle of $\sim$50° between the membrane surface and the O-P-O$^-$ plane (Yeagle, 1978). Dehydration inclines the headgroup toward the membrane surface (Büldt et al., 1979). The flexibility and disorder increase toward the trimethylammonium group (Browning, 1981), and headgroup ordering decreases with progressive hydration (Bechinger and Seelig, 1991; Ulrich and Watts, 1994). Moreover, our data are in good agreement with previous IR dichroism data on PC-headgroup orientation (Fringeli and Gunthard, 1981; Akutsu et al., 1981; Ter-Minassian-Sara et al., 1988; Holmgren et al., 1987; Okamura et al., 1990; Hübner and Mantsch, 1991).

Besides these general properties, our results show subtle modifications of headgroup orientation of DODPC, correlating with changes in the bilayer dimensions. With progressive dehydration the area requirement per lipid as well as the disorder of the PC headgroup orientation decrease. After transformation from the gel into the SG_I phase, the raised A_L, decreased d_{pol}, and the sharpening of the maxima of the electron density profile are accompanied by an almost parallel alignment of the PC moiety along the membrane plane. Obviously, a larger surface area makes it easier for the trimethylammonium group to move closer to the hydrocarbon boundary and to displace water from the headgroup. This tendency implies a close approach between the phosphate and ammonium groups of neighboring molecules at low hydration levels to minimize the distance between the groups of opposite charge. The antisymmetrical stretching mode of the ammonium methyl groups, $\nu_{as}(CH_3)_{Chol}$, was found to be sensitive to direct phosphate-ammonium interactions (Grdadolnik et al., 1991). In DODPC the $\nu_{as}(CH_3)_{Chol}$ band shifts, from $\sim$3029 cm^{-1} measured in the gel state, down to $\sim$3026 cm^{-1} in the subgels (see Fig. 8). We conclude that this change is caused by the appearance of relatively strong interactions between the phosphate oxygens and the methyl hydrogens, in analogy to the interpretation of similar effects in phosphocholine reversed micelles and multilayers (Grdadolnik et al., 1991). The strong perpendicular dichroism (i.e., $2 \times A_\perp > A_\parallel$) of the $\nu_{as}(CH_3)_{Chol}$ band observed in the SG_I state indicates, in agreement with the behavior of the dichroism of the C-N modes, the immobilization of the terminal trimethylammonium group. This effect weakens in the SG_{II} phase and disappears completely upon transformation of the lipid into the L_α phase. The drastic shift of the centers of gravity of the phosphate vibrations in the subgels (Binder et al., 1997) (cf. also Fig. 5) can also be assumed to reflect direct phosphate-ammonium interactions, which stabilize a rigid arrangement of the PC headgroups upon the removal of water ($R_{W/L} < 4$).

Frequency shifts of the ν_{as}(C-N) and ν_s(C-N) bands suggest conformational changes in the choline group in the subgels of DODPC (Binder et al., 1997). Similar results are obtained upon crystallization of DMPC at low RH values by means of Raman spectroscopy (Kint et al., 1992). X-ray investigations showed that in PC crystals, the ammonium group folds back toward the phosphate group, thus realizing a close intramolecular approach between both moieties (Pearson and Pascher, 1979). Although it is well established that the *trans-gauche* equilibrium of O-C-C-N can be controlled in the crystalline state by RH, the fraction of the respective conformers cannot be extracted from the IR spectra at present, because of unknown extinction coefficients of the respective IR bands (Fringeli and Gunthard, 1981).

Ordering of adsorbed water

In the previous paper (Binder et al., 1997) we qualitatively analyzed the ν_{13}(OH) absorption band of water adsorbed onto DODPC, in terms of the binding strength of H-bonds formed with the PC headgroup. In particular, the sharpening of this band in the SG_I phase was attributed to an almost uniform population of water molecules interacting with a small number of binding sites at the lipid. Fig. 9 *c* indicates that this effect is accompanied by a marked perpendicular dichroism of the ν_{13}(OH) band. The apparent IR order parameter, $S_{IR}(\nu_{13}(OH))$, was obtained by integration of the polarized ν_{13}(OH) bands in the spectral range between 3200 and 3600 cm^{-1} (cf. Eq. 1). The nonzero value of $S_{IR}(\nu_{13}(OH))$ (Fig. 10 *b*, ν_{13}) observed at low RH in the SG_I phase indicates a high degree of molecular ordering, which is correlated with the narrow ν_{13}(OH)-bandshape (Fig. 10 *a*). With increasing RH, the increase of the bandwidth, $\Delta\nu_{13}$(OH), indicates a more heterogeneous distribution of interaction strengths of the water, leading to a marked decrease in the absolute value of $S_{IR}(\nu_{13}(OH))$. Hence, in the subgels the IR order parameter behaves in a manner that is very similar to that of the width of the ν_{13}(OH) band with increasing RH. In the L_α and gel states $\Delta\nu_{13}$(OH) decreases with dehydration, but in contrast to the subgels, only low water ordering was detected in the whole RH range by

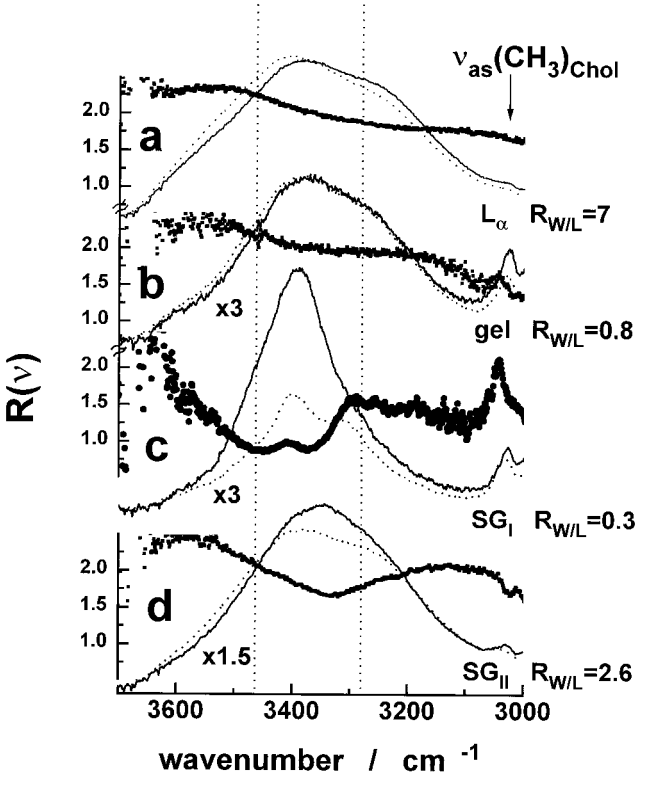

FIGURE 9 Polarized absorbance spectra, $A_\parallel(\nu)$ (*dotted curve*), and $2 \times A_\perp(\nu)$ (*solid curves*), and spectra of the corresponding dichroic ratio, $R(\nu) = A_\parallel(\nu)/A_\perp(\nu)$ (*scatter curves*), of the ν_{13}(OH) stretching region of water adsorbed to DODPC in different phases. $R(\nu)$ is quantified at the left coordinate axes. The vertical dotted lines indicate the central positions of the wavenumber ranges used for the calculation of $S_{IR}(\nu_{3280})$ and $S_{IR}(\nu_{3460})$. The position of the antisymmetrical C-H stretching mode of the trimethylammonium groups is indicated at the top. The absorption spectra of the rigid states are amplified by the factors given in the figure.

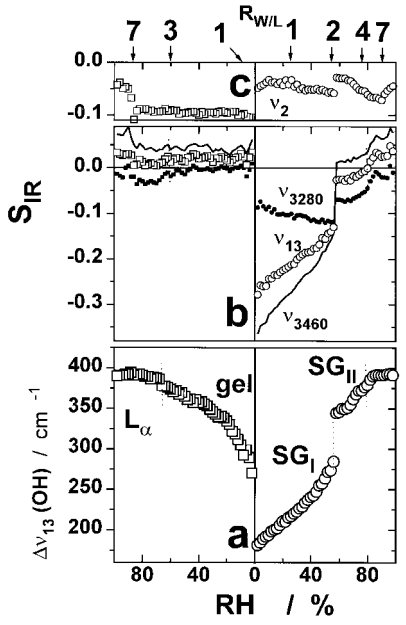

FIGURE 10 Full width at half-maximum intensity, $\Delta\nu_{13}$(OH) (*a*), and infrared order parameter, S_{IR}, of the OH stretching, band, ν_{13} (*b*), and S_{IR} of the bending band, ν_2 (*c*), of water adsorbed to DODPC as a function of relative humidity. In *b* the curves denoted as ν_{3280} (*small solid squares*) and ν_{3460} (*line*) are infrared order parameters calculated at the right and left flank of ν_{13}(OH), respectively (centered around the *vertical dotted lines* in Fig. 9; see text). Selected $R_{W/L}$ values are shown at the top axis. Vertical dotted lines indicate phase boundaries.

means of the IR order parameter, which adopts values near zero.

Inspection of the polarized IR spectra clearly indicates that in all cases the dichroism changes across the wavenumber range of the ν_{13}(OH) band (Fig. 9). This effect is filtered out in the spectrum of the dichroic ratio, $R(\nu) = A_{\parallel}(\nu)/A_{\perp}(\nu)$, which indicates several populations of transition moments with different mean orientations. It turns out that in the L_α, gel, and, to some extent, in the SG_{II} states, the ν_{13}(OH) band is slightly parallel polarized ($R > 2$, $S_{IR} > 0$) at its left flank and slightly perpendicularly polarized ($R < 2$, $S_{IR} < 0$) at its right flank. In the SG_I phase at a very low level of hydration, the band is clearly perpendicularly polarized at wavenumbers greater than 3350 cm^{-1} (Fig. 9 *c*). A less polarized shoulder appears, however, at ~3300 cm^{-1}. At hydration on the order of $R_{W/L} = 2$–3 (SG_{II}), the additionally adsorbed water molecules obviously decrease the perpendicular polarization at both flanks.

To quantify these tendencies, we calculate the IR order parameters in restricted spectral ranges at higher ((3460 ± 40) cm^{-1}) and lower ((3280 ± 20) cm^{-1}) wavenumbers, yielding $S_{IR}(\nu_{3460})$ and $S_{IR}(\nu_{3280})$, respectively (Figs. 8 and 9). The two order parameters show parallel courses in the L_α, gel, and SG_{II} states. In the SG_I phase it turns out that the increase in the mean value $S_{IR}(\nu_{13}(OH))$ is caused solely by the apparent dichroism of the central and high wavenumber region of ν_{13}(OH), whereas the dichroism of the right flank remains nearly constant or even decreases slightly.

An unambiguous assignment of the different spectral regions of the ν_{13}(OH) band seems to be impossible, owing to its complicated structure, consisting of overlapping, highly coupled symmetrical (ν_1) and antisymmetrical (ν_3) OH-stretching vibrations, originating from free and hydrogen-bound water molecules, as well as from a Fermi resonance band that is induced by the coupling between OH-stretching and the second overtone of the H_2O-bending mode, $\nu_2(H_2O)$, at ~1650 cm^{-1} (Zundel, 1969; Wong and Whalley, 1975; McGraw et al., 1978; Sceats et al., 1979). Assuming that the OH-absorption frequency is exclusively related to the binding strength of the respective water molecules, the wavelength-dependent dichroism of the ν_{13}(OH) band simply reflects different orientations of the water molecules interacting with different sites on the lipid.

However, this treatment ignores the spectral smearing between the coupled ν_1 and ν_3 modes, and therefore it can distort the interpretation of the basic dichroic features of the ν_{13}(OH) band in terms of water ordering. At a low level of hydration, the few water molecules adsorbed onto DODPC interact predominantly with the lipid, and therefore the interpretation of the spectrum in terms of free molecule parentage seems to be appropriate. The two clearly resolved maxima evident in the parallel polarized ν_{13}(OH) band in the SG_I phase are separated by 90 cm^{-1}, which amounts roughly to the frequency shift expected between the ν_1 and ν_3 modes (100–150 cm^{-1}; Zundel, 1969). Note that the OH-stretching band of water is known to become structured upon interaction of the water with polyatomic ions, because of their (water-) structure-breaking ability (Walrafen, 1971). At a higher degree of hydration we can use the results of IR and Raman studies on amorphous "glassy" water and polycrystalline ice (Wong and Whalley, 1975; McGraw et al., 1978; Bergren et al., 1978). These detailed analyses show that the low- and high-frequency edges of the ν_{13}(OH) band correspond to mixed OH-stretching fundamentals with a high fraction of symmetrical intramolecular vibrations, in which the ν_1 modes of neighboring molecules are either in or out of phase, respectively. This assignment is confirmed by the polarized Raman spectrum of films of glassy water (Li and Devlin, 1973).

In view of these results, we assume for a rough estimation that the low wavenumber flank of the ν_{13}(OH) band refers to a "ν_1-like" mode, the dichroism of which reflects the average orientation of the symmetry axis of the water molecules. This assignment is supported by the observation that in the whole RH range, and specifically in the SG_I phase and at the SG_I-SG_{II} transition, the order parameter $S_{IR}(\nu_{3280})$ behaves like $S_{IR}(\nu_2)$, the IR order parameter of the $\nu_2(H_2O)$ mode (cf. Fig. 9, *b* and *c*), the transition moment of which can be assumed to point parallel to that of ν_1. However, a detailed quantitative comparison of $S_{IR}(\nu_{3280})$ and $S_{IR}(\nu_2)$ is not appropriate, because the $\nu_2(H_2O)$ band is strongly distorted by overlapping bands (C═O and C═C stretching; Binder et al., 1997).

On the basis of these assignments, the negative S_{IR} values measured in the SG_I phase across the ν_{13}(OH) band and, in

particular, at its right flank ($S_{IR}(\nu_1) \approx S_{IR}(\nu_{3280}) \approx -0.1$) indicate that the permanent dipole moment of the few waters adsorbed onto the lipid preferentially orients parallel to the bilayer surface. With progressive hydration, the only small increase in the $S_{IR}(\nu_{3280})$ and $S_{IR}(\nu_2)$ gives rise to the hypothesis that the mean dipole orientation remains nearly constant, except for a slight inclination away from the bilayer plane parallel to the reorientation of the PC group (Fig. 9, *b* and *c*, and Fig. 8 for illustration). Thus the infrared dichroism of the OH-stretching region indicates a strong cooperation between the PC headgroup orientation and water ordering, in agreement with recent IR dichroism measurements of the ν_2 band of water bound to DPPC at various degrees of hydration (Okamura et al., 1990). The negative values of $S_{IR}(\nu_{3280})$ and $S_{IR}(\nu_2)$ suggest that the permanent water dipole is oriented, with respect to the membrane surface, like the headgroup dipole (see previous paragraph), and thus both dipoles can be assumed to point antiparallel on the average. Computer studies have given evidence that in the vicinity of phospholipid headgroups, water builds highly structured regions that tend to compensate the headgroup dipole moment (Klose et al., 1985; Binder and Peinel, 1985; Peinel et al., 1983; Zhou and Schulten, 1995).

However, the interpretation of the IR order parameters in terms of mean orientations without considering the distribution of water orientations yields an incomplete picture of the properties of water adsorbed onto surfaces. Fixed relations between the order parameters of the ν_1 and ν_3 modes hold for the limiting case of free rotations about one of the three principal axes of an isolated water molecule, namely, $S_{IR}(\nu_1) = -2\ S_{IR}(\nu_3)$ (axis 1 in Fig. 8), $S_{IR}(\nu_1) = -0.5 S_{IR}(\nu_3)$ (axis 2, i.e., $|S_{IR}(\nu_3)| > |S_{IR}(\nu_1)|$, see below), and $S_{IR}(\nu_1) = S_{IR}(\nu_3)$ (axis 3). If one attributes the left flank of the ν_{13}(OH) band to a "ν_3-like" mode, the negative $S_{IR}(\nu_{3460})$ and $S_{IR}(\nu_{3280})$ data measured in the SG_I phase indicate that the HOH plane of the first membrane-bound water molecules aligns parallel, on the average, to the membrane surface. The marked difference between both IR order parameters with $|S_{IR}(\nu_{3460}) \approx S_{IR}(\nu_3)| > |S_{IR}(\nu_{3280}) \approx S_{IR}(\nu_1)|$ can be explained by a broad distribution of water orientations about the axis parallel to H-H (axis 2). In this case a considerable fraction of water dipoles can be assumed to deviate from their antiparallel alignment with respect to the headgroup dipole. A molecular dynamics simulation of water ordering on lipid headgroups (Peinel et al., 1983) showed that the orientations of the first water molecules ($R_{W/L} < 4$) bound to the headgroups are determined only partially by the direction of the headgroup dipole, but still more so by the position of the water binding sites on the lipid, i.e., the phosphate and the possibly of the carbonyl group as well. Water bridges between the phosphate groups and/or highly oriented H-bonds to the carbonyl groups of DODPC were suggested previously (Binder et al., 1997).

The drastic increase in $S_{IR}(\nu_{3460})$, from $S_{IR}(\nu_{3460}) < -0.2$ (SG_I) up to small positive values (<0.09) in the SG_{II}, gel, and L_α states, indicates that the ordering of the water decreases with progressive hydration (Fig. 10 *b*). Moreover, the quadrupolar splitting of deuterated water determined by means of NMR ends up with a tiny order parameter of $S_{NMR} \approx 0.01$–0.02 when compared with the value of completely immobile water, even for the first hydration shell of PC lipids (Klose et al., 1985; Gawrisch et al., 1992; Volke et al., 1994). The small S_{NMR} values were attributed to the dynamic averaging over flipping motions of the water molecules around their symmetry axis (1 in Fig. 8), which are rapid in the NMR time scale ($\sim 10^{-5}$ s) (Gawrisch et al., 1992). This type of reorientation was already detected in molecular dynamics simulations of water rotational diffusion in the vicinity of lipid headgroups (Binder and Peinel, 1985). In the time scale of infrared absorption ($<10^{-11}$ s), the averaging of water orientations possesses a preferentially static character in comparison with the correlation time for water reorientation of $\sim 10^{-12}$ s (Binder and Peinel, 1985). Hence a mechanism considering only flipping motions about the dipole axes of the water molecules is sufficient to explain small values of the IR order parameter $S_{IR}(\nu_{3280})$, only in the case in which this axis includes nearly the magic angle with the membrane normal. Otherwise, reorientations about all principal axes of the water molecule should be assumed to be in accordance with theoretical results (Binder and Peinel, 1985).

Area compressibility

The lyotropic phase behavior of DODPC can be understood in terms of the osmotic pressure, Π, acting on the lipid bilayers at a given RH:

$$\Pi = -\frac{k_B \cdot T}{v_w} \cdot \ln\left(\frac{RH}{100}\right) \tag{8}$$

where k_B, T, and v_W denote the Boltzmann constant, the absolute temperature, and the molecular volume of water, respectively (Parsegian et al., 1979; Rand, 1981; Rand and Parsegian, 1989). Hence, with decreasing RH the multilamellar stacks of bilayers are exposed to an increasing Π, leading to their compression, i.e., the gradual change of A_L, d_L, and d_W. Because the Luzzati formalism assumes volumetrically incompressible lipids (and water), only two geometric variables are independent, namely A_L and d_W.

Fig. 11 *a* shows the area per DODPC molecule, A_L, which depends on the isotropic lateral pressure,

$$|\tau| = \Pi \cdot d_w, \tag{9}$$

applied to the bilayer (Rand, 1981; Rand and Parsegian, 1989; Koenig et al., 1997). Upon dehydration the lateral pressure, $|\tau|$, increases monotonously up to values of ~ 35 mN/m in the low hydrated gel state. Within the error limits the relation between $|\tau|$ and A_L remains nearly linear in the whole A_L range, i.e., there is no significant rise in the slope, and thus no bilayer elasticity limit for compression is detected, as is typically found in the case of the compression of lipid monolayers at the air/water interface. The transfor-

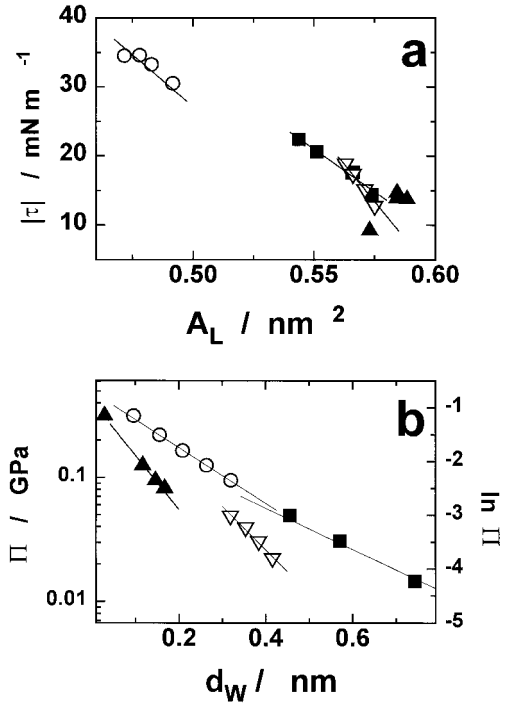

FIGURE 11 Lateral pressure, $|\tau|$, as a function of the area per lipid, A_L (*a*), and osmotic pressure, Π, as a function of the distance between opposite bilayers, d_W (*b*). Symbols denote the experimental data obtained from the x-ray measurements for the different phases: L_α (■), gel (○), SG_I (▲), and SG_{II} (▽). The lines represent linear regressions. Slopes and intercepts are given in Table 2 in terms of K_a and A_0 (*a*) and λ and Π_0 (*b*) (see text).

mation into the subgels reduces $|\tau|$ from ~30 mN/m to ~15 mN/m. The almost linear changes in the IR order parameters of the PC moiety of DODPC upon dehydration indicate a continuous increase in the molecular order in the region of the headgroups in the L_α and gel states, and thus correlate with the almost linear dependence of $|\tau|$ versus A_L.

Using a first-order approximation,

$$|\tau| = -K_a \cdot \frac{(A_L - A_0)}{A_0} \qquad (10)$$

one obtains the mean isothermal elastic area compressibility modulus of the membrane, K_a, as well as an estimation of the area per lipid in the relaxed (i.e. fully hydrated) state, A_0, by linear regression of the $|\tau|$ values measured in the respective phases versus A_L (Table 2). In the SG_I phase it is not appropriate, however, to apply Eq. 10, because of the scattering of the few data and the narrow A_L range.

Membrane compressibility may be translated into the free volume available in the membrane. Polyunsaturation of lipid acyl chains is known to increase lateral compressibility (i.e., to decrease K_a) by means of the free volume created by the double bonds (Koenig et al., 1997; Straume and Litman, 1987). The compressibility modulus of DODPC in the L_α phase adopts values in the order of those typically observed in liquid-crystalline PCs (Table 2). Hence the diene groups have almost no effect on the packing density in the liquid-crystalline bilayers of DODPC compared with disaturated lipids. Obviously, the *trans*-butadiene units fit well within the bilayer at a position near the polar/apolar interface.

The lateral compressibility modulus of the bilayer, K_a, can be assumed to be caused by the resistance of the bilayer against compression in the region of the headgroups and of the hydrophobic core. In the L_α phase the methylene chains and the headgroups are relatively loosely packed because of the high degree of disorder. The gradual lateral compression of the bilayer will progressively restrict the conformational freedom of the polar and apolar parts of the molecules (cf. Fig. 4). Consequently, K_a can be thought to reflect predominantly entropic effects, which refer to the work needed to diminish the free volume in the bilayer.

At the L_α-gel transition, the freezing of the polymethylene chains is expected to change fundamentally the situation in the hydrophobic core. Now the methylene segments are in the extended all-*trans* conformation with a reduced cross section, in which a further response by means of segmental ordering is nearly impossible. The area requirement of the PC headgroup can be assumed to be the limiting factor acting against lateral compression of the membranes. Hence the steric repulsion between the headgroups is expected to

TABLE 2 Area compressibility modulus of the membranes, K_a, and decay length, λ, of the repulsive force between opposite bilayers of DODPC in different phases

Phase	L_α	gel	SG_I	SG_{II}	L_α/Ref.	gel/Ref.
K_a (mN · m^{-1})	160	180	—	300	145,* 121[#]	855*
A_0 (nm^2)	0.64	0.59	—	0.60	0.62–0.68[§]	0.47–0.53[§]
λ (nm)	0.23	0.19	0.10	0.12	0.20–0.22[¶]	0.12–0.13[¶]
Π_0 (GPa)	0.35	0.52	0.42	0.67		0.80–0.11[‖]
w_{dehyd} (kJ · mol^{-1})	13	14	7	13		

K_a and λ are obtained from the slopes of regression lines shown in Fig. 11, *a* and *b*, respectively. The intercepts yield a rough estimate of the area per lipid in the relaxed state, A_0, and the osmotic pressure, Π_0, at close contact ($d_w = 0$) between the bilayers. Some reference data are given for comparison. w_{dehy} denotes the work of complete dehydration of the lipid (see text).

*DMPC at 29°C (L_α) and 8°C (gel) (area expansion modulus measured by means of micromechanical manipulation) (Evans and Needham, 1987).

[#]DMPC-d54 (L_α) at 30°C (area compression modulus) (Koenig et al., 1997).

[§]Disaturated PCs in excess water (Rand and Parsegian, 1989), and references cited therein).

[¶]Disaturated PCs (Rand and Parsegian, 1989; McIntosh and Simon, 1993).

[‖]PE-lipids (Rand and Parsegian, 1989).

**SE: ±60 (K_a), ±0.03 (λ), and ±0.2 (Π_0) in the units indicated in the first row.

increase the compressibility modulus markedly. However, K_a remains almost unchanged after transformation of DODPC into the gel state.

A comparison of the lyotropic phase behavior of DODPC and disaturated PCs as, e.g., DMPC shows that the diene groups promote the formation of subgels that are characterized by a paraffin-like arrangement of tilted polymethylene chains with strongly damped reorientations about their long axes, as indicated by the appearance of the correlation field splitting of the CH_2 bending and rocking vibrations (Binder et al., 1997). In the metastable gel state preceding the subgels, no correlation field splitting was detected. This finding indicates that the all-*trans* acyl chains are disordered with respect to rotations about their long axes, and consequently their cross section perpendicular to the chain axes increases slightly, as observed by wide-angle x-ray measurements. Possibly these different arrangements of the all-*trans* octadecadienoyl chains cause the different compressibility moduli measured in the gel and subgel states.

Note that even in the subgels, K_a remains significantly smaller than that obtained in the gel state of DMPC ($L_{\beta'}$ phase) by means of micromechanical manipulation (Evans and Needham, 1987; see Table 2). Although the frozen chains cannot approach one another much more closely, they can change tilt on compression to decrease their surface area. This degree of freedom is possibly responsible for the small lateral pressure, $|\tau|$, observed in the SG_I phase, which possibly indicates the almost relaxed molecular packing within the membrane plane. The correspondingly high area requirement $A_L \approx 0.57-0.59$ nm^2 enables the nearly flat alignment of the PC group parallel to the bilayer surface, with direct interactions between the phosphate and trimethylammonium groups, as indicated by the IR measurements. Hence effectively neighboring headgroups do not repel each another, and thus this lateral interaction gives no or even a negative (attractive) contribution to K_a. We suggest that this headgroup arrangement is caused by the dense packing of the tilted acyl chains in the subgels.

Recently the osmotic stress technique was shown to yield reasonable lateral compressibility data, using x-ray measurements in the intermediate range of lipid hydration, with $R_{W/L} \approx 10-20$ (Koenig et al., 1997). The water directly bound to the lipid must be viewed as an inherent constituent of the membrane, and consequently, at low hydration ($R_{W/L} < 4$), the implicit assumptions of nonpenetrating lipid and water layers are expected to introduce systematic errors of the geometric parameters A_L and d_w and thus to affect K_a. Furthermore, the molecular arrangement of the acyl chains and of the lipid headgroup changes distinctly with progressive dehydration, and consequently the assumption of incompressible molecules implicit in Eq. 9 does not hold. For example, the density of lipids in the L_α and gel phases differs by more than 5% (Rand and Parsegian, 1989). The corresponding change in the volume per lipid ($\sim$0.04 nm^3) is on the same order as the volume of the water adsorbed onto the lipid at $R_{W/L} < 2$ ($<$0.06 nm^3). In addition, at low RH the precise value of the molar volume of water is still an open question, as it has not been measured directly (McIntosh et al., 1987). The moderate changes in the headgroup order parameters observed in each single phase range of DODPC give rise, however, to the conclusion that within these boundaries the density remains constant to a good approximation. We analyzed the x-ray diffraction data for each phase separately, assuming a standard density of 1 g/cm^3. Thus our basic results are related to well-pronounced structural differences between the different phases of DODPC that may possibly be modified but not altered on principle by a refinement of the treatment.

Repulsive forces between the bilayers

The functional dependence between the osmotic pressure and the thickness of the water layer between opposite bilayers in multilamellar lipid samples is usually well fitted by the exponential decay law (Rand, 1981; Rand and Parsegian, 1989),

$$\Pi = \Pi_o \exp(-d_w/\lambda). \quad (11)$$

Fig. 11 *b* shows that this dependence can also be applied to the respective DODPC data, yielding decay lengths of $\lambda = 0.20-0.23$ nm in the gel and L_α states and $\lambda = 0.10-0.12$ nm in the subgels (Table 2). The data of the subgels reflect the reduced hydration, a typical property of solid PC lamellae and of lipids with PE headgroups (Rand and Parsegian, 1989; McIntosh and Simon, 1993). This decrease in the decay length, λ, can be explained by an increase in the lateral order in the headgroup region preventing water adsorption. The headgroup structure is distinctly enhanced in PE bilayers by lateral hydrogen bonds formed between the PE groups. However, in PEs and crystalline disaturated PCs, the smaller capacity of water adsorption is accompanied by a reduced area requirement of the headgroups, in contrast to DODPC, where A_L even increases.

The small decay length in the subgels means that a smaller osmotic pressure should be applied than in the gel state, to keep the bilayer surfaces at a constant d_W. This finding correlates with the small lateral tension observed in the subgels, and gives rise to the conclusion that the bilayers are obviously less stressed in the subgels, laterally as well as perpendicularly with respect to the surface, than in the gel state.

Several factors potentially contribute to the repulsion between lipid bilayers: 1) water structure in the vicinity of the lipid headgroups, 2) headgroup conformation and mobility, and 3) individual and collective motions of the whole lipid molecules (see Leikin et al., 1993, for a review). The latter effects give rise to undulation, protrusion, and peristaltic forces, which typically arise between fluid bilayers at larger separations ($d_w > 2$ nm) (Helfrich, 1978; Israelachvili and Wennerström, 1992). It can be assumed that the lipid multilayers are constrained by the underlying solid substrate, which suppresses these forces in the gel and subgel states. The almost equal decay lengths measured in

the L_α and gel states of DODPC suggest that this assumption also applies to the liquid-crystalline phase at low hydration.

Solvation models of lipid hydration, 1), predict that water ordering near the membrane surface (Marcelja and Radic, 1976), as well as an ordered arrangement of the lipid polar groups (Kornyshev and Leikin, 1989), can induce strong repulsive forces. An important consequence of the latter model is that the more orderly the in-plane packing of the polar heads, the shorter the decay length. In DODPC we found indeed that in the subgels where the IR order parameters indicate a higher degree of water and headgroup ordering (and in particular their flat in-plane alignment), the decay length, λ, is shorter than in the gel state.

An alternative model, 2), concentrates on a sort of "chemical" hydration of the membrane surface (Cevc, 1991). It assumes that the interfacial repulsion depends much more on the interfacial characteristics and dynamics than on solvent properties (see also Israelachvili and Wennerström, 1992). Within the frame of this model, the larger λ values of DODPC in the gel and L_α states reflect the higher orientational freedom of the PC headgroup when compared with its highly ordered packing in the subgels, especially in the SG_I phase. Cevc (1991) derived an exponential decay law of Π in which the preexponential factor, Π_0, is proportional to $(\sigma_p/d_p)^2$ (cf. Eq. 7; in Cevc, 1991, d_p is the interfacial thickness). For the surface charge density, σ_p, one can assume that $\sigma_p \propto A_L^{-1}$, and $d_p \approx d_{pol}$. One obtains $(\sigma_p/d_p)^2 \propto (d_{pol} \times A_L)^{-2} \approx v_{pol}^{-2}$, where v_{pol} is the molecular volume of the polar part of the bilayer. For incompressible headgroups, i.e., v_{pol} = constant, one expects a constant Π_0, as really found in the rigid states of DODPC within the experimental error (Table 2).

McIntosh and Simon (1993) decomposed the repulsive forces between DPPC bilayers in the subgel phase into a very-short-range and short-range component with decay lengths of 0.007 nm and 0.14 nm, respectively. The former, acting at $d_w < 0.4$ nm, was attributed to steric repulsion between opposing headgroups, which are suggested to extend slightly farther into the water layer for subgel than for gel bilayers. A similar steep increase of the repulsive interaction was not detected in the DODPC samples, possibly owing to the smaller interfacial thickness of the DODPC bilayer with in-plane oriented PC groups.

The integrated work of lipid dehydration per monolayer can be roughly estimated on the basis of the empirical decay law of the hydration force by $w_{dehyd} \approx 0.5 \times N_A \times \Pi_0 \times \lambda \times A_{min}$ (Rand and Parsegian, 1989), where A_{min} denotes the area per lipid at low water content. The factor 0.5 accounts for the fact that the force (Eq. 11) acts between two opposite surfaces. Using typical values of the area per lipid, A_{min} = 0.55 nm^2 (L_α), 0.47 nm^2 (gel), and 0.57 nm^2 (subgels), and the contact pressures, Π_0, and the decay lengths, λ, given in Table 2, one obtains an estimate of the (hypothetical) work that would be necessary to dehydrate DODPC bilayers existing in the different states. Note that this treatment ignores the phase transitions appearing upon dehydration of the L_α and SG_{II} states, and thus it extrapolates the work necessary to remove water down to complete dehydration, preserving at the same time the structural properties of the respective phase. For the L_α, gel, and SG_{II} states, one obtains w_{dehyd} = 13–14 kJ/mol, but only about one-half of this value for the SG_I phase (cf. Table 2). This finding correlates with the degree of water and headgroup ordering, which is low in the L_α, gel, and, to some extent, the SG_{II} states, but is relatively high in the SG_I phase. Note that w_{dehyd} equals the free energy of dehydration, representing a measure of the thermodynamic costs to remove the water from the lipid + water system. The preference of the polar region of the bilayer to be hydrated is indicated by the relatively high values of w_{dehyd} measured in the L_α, gel, and SG_{II} states. These costs of free energy are compensated partially in the SG_I state by a gain of free energy, which is caused by the favorable arrangement of the headgroups, of water structuring, but also by the dense packing of the acyl chains with a maximum of attractive van der Waals contacts. It can be suggested that the water-lipid interactions that are broken up upon desorption of water are partially replaced by direct interactions between the lipid headgroups. From a thermodynamic point of view, the approach of two bilayers in the SG_I phase is less expensive and thus results in a weaker repulsion (shorter decay length λ) between opposite bilayers as the approach of the membranes in the L_α, gel, or SG_{II} states.

The present paper deals with PC headgroup properties and ignores the carbonyl groups representing a potential hydration site of DODPC (Binder et al., 1997). Gawrisch et al. (1992) found that the influence of carbonyls on lipid hydration is minor in comparison with the influence of the other parts of the polar group. The position of the C═O stretching band of DODPC changes drastically in the subgel phases, either because of close contact interactions between the lipids or because of the existence of well-oriented H-bonds with water (Binder et al., 1997). Even in the latter case, i.e., if the carbonyl groups participate in primary hydration, our conclusions about the interrelation between λ and headgroup and water orderings are not affected on principle.

SUMMARY AND CONCLUSIONS

The combination of x-ray diffraction and infrared linear dichroism data gives insight into the interrelation between the structure of the polar region of the bilayer and the overall dimensions of the membrane. The area requirement per DODPC within the membrane plane, A_L, is determined mainly by the packing properties of the octadecadienoyl chains in the different states that adopt DODPC, depending on RH.

In the subgel phase, SG_I, the DODPC molecules occupy a relatively high area, probably because of conformational restrictions in the vicinity of the dienic groups, which induce a permanent tilt of the acyl chains to become densely

packed. As a result, the PC headgroups adopt an almost in-plane orientation owing to intermolecular interactions that involve the trimethylammonium and phosphate groups, as well as highly ordered water molecules. The structured and, to a great extent, dehydrated membrane surfaces repel each another much more weakly than membranes that are in the metastable gel state at identical intermembrane separations. In this case the area requirement per lipid is smaller, and the extent of the headgroups in the direction perpendicular to the membrane plane bigger than in the subgels, because of the relatively loose packing of the frozen acyl chains.

In the SG_I phase the dehydration of the membranes requires less work, and thus it represents the more favorable state in a thermodynamic sense than the gel at identical RH. As a consequence, the repulsive force drops more steeply in the subgels with increasing interbilayer separation. These results confirm the idea of a "chemical hydration." It states that in many instances the most important reason for the existence of hydration force is direct headgroup-water, water-water, and headgroup-headgroup interactions (Cevc, 1991; see also Zhou and Schulten, 1995).

The phase transformations of DODPC observed with changing RH indicate that the system tends to avoid stress in the lateral as well as the perpendicular direction by modifications of molecular conformations and packing properties. The compression moduli of the rigid states of DODPC are not extensively greater than that of the liquid-crystalline phase.

The present paper is not subjected to the details of the arrangement of the octadecadienoyl chains and, in particular, to the conformations in the region of the diene and carbonyl-ester groups. A detailed analysis of the chain packing modes will be given separately. The interpretation of the ν_{13}(OH) band of water adsorbed to the lipid seems to be plausible, in view of assignments given in the literature. However, this point should be verified in lipid systems by further experimental work that is now in progress.

We thank D. P. B. Kohlstrunk for the humidity control and Ms. U. Staudte, who made the x-ray measurements.

This work was supported by the Deutsche Forschungsgemeinschaft under grant SFB294.

REFERENCES

Akutsu, H. 1981. Direct determination by Raman scattering of the conformation of the choline group in phospholipid bilayers. *Biochemistry.* 20:7359–7366.

Akutsu, H., M. Ikematsu, and Y. Kyogoku. 1981. Molecular structure and interaction of dipalmitoyl phosphatidylcholine in multilayers. Comparative study with phosphatidylethanolamine. *Chem. Phys. Lipids.* 28: 149–158.

Bechinger, B., and J. Seelig. 1991. Conformational change of the phosphatidyl head group due to membrane hydration. *J. Chem. Phys. Lipids.* 58:1–5.

Bergren, M. S., D. Schuh, M. G. Sceats, and S. A. Rice. 1978. The OH-stretching region infrared spectra of low density amorphous solid water and polycrystalline ice Ih. *J. Chem. Phys.* 69:3477–3482.

Binder, H., A. Anikin, B. Kohlstrunk, and G. Klose. 1997. Hydration induced gel states of the dienic lipid 1,2-bis(2,4-octadecadienoyl)-sn-glycero-3-phosphorylcholine and their characterization using infrared spectroscopy. *J. Phys. Chem. B.* 101:6618–6628.

Binder, H., and G. Peinel. 1985. Behaviour of water at membrane surfaces—a molecular dynamics study. *J. Mol. Struct. (Theochem.).* 123: 155–163.

Blume, A. 1991. Phase transitions of polymerizable phospholipids. *Chem. Phys. Lipids.* 57:253–273.

Browning, J. L. 1981. Motions and interactions of phospholipid head groups at the membrane surface. 1. Simple alkyl head groups. *Biochemistry.* 20:7144–7151.

Büldt, G., H. U. Gally, J. Seelig, and G. J. Zaccai. 1979. Neutron diffraction studies on phosphatidylcholine model membranes. I. Head group conformation. *J. Mol. Biol.* 134:673–691.

Cevc, G. J. 1991. Hydration force and the interfacial structure of the polar surface. *Chem. Soc. Faraday Trans.* 97:2733–2739.

Cevc, G., and D. Marsh. 1987. Phospholipid Bilayers, Physical Principles and Models. John Wiley and Sons, New York.

Derreumaux, P., K. J. Wilson, G. Vergoten, and W. L. Peticolas. 1989. Conformational studies of neuroactive ligands. 1. Force field and vibrational spectra of crystalline acetylcholine. *J. Phys. Chem.* 93: 1338–1350.

Dluhy, R. A., B. Z. Chowdhry, and D. G. Cameron. 1985. Infrared characterization of conformational differences in the lamellar phase of 1,3-dipalmitoyl-sn-glycero-2-phosphatidylcholine. *Biochim. Biophys. Acta.* 821:437–444.

Evans, E., and D. Needham. 1987. Physical properties of surfactant bilayer membranes: thermal transitions, elasticity, rigidity, cohesion, and colloidal interactions. *J. Phys. Chem.* 91:4219–4228.

Fringeli, U. P. 1977. The structure of lipids and proteins studied by attenuated total reflection infrared spectroscopy. Oriented layers of a homologous series of phosphatidylethanolamine to phosphatidylcholine. *Z. Naturforsch.* 32c:20–45.

Fringeli, U. P., and H. H. Gunthard. 1981. Infrared membrane spectroscopy. *Mol. Biol. Biochem. Biophys.* 31:270–332.

Gawrisch, K., D. Ruston, J. Zimmerberg, V. A. Parsegian, R. P. Rand, and N. Fuller. 1992. Membrane dipole potential, hydration forces, and the ordering of water at membrane surfaces. *Biophys. J.* 61:1213–1223.

Good, B. S., P. C. Taylor, A. J. Hopfinger. 1981. Theory of structure and conformation of polyacetylene. *J. Appl. Phys.* 52:6008–6010.

Grdadolnik, J., J. Kidric, and D. Hadzi. 1991. Hydration of phosphatidylcholine reversed micelles and multilayers—an infrared spectroscopic study. *Chem. Phys. Lipids.* 59:57–68.

Harrick, N. J. 1967. Internal Reflection Spectroscopy. Wiley, New York.

Helfrich, W. 1978. Steric interactions of fluid membranes in multilayer systems. *Z. Naturforsch.* 33a:305–315.

Holmgren, A., B.-A. Johanson, and G. Lindblom. 1987. An FT-IR linear dichroism study of lipid membranes. *J. Phys. Chem.* 91:5298–5301.

Hsieh, C.-H., S.-C. Sue, P.-C. Lyu, and W.-G. Wu. 1997. Membrane packing geometry of diphytanoylphosphatidylcholine is highly sensitive to hydration: phospholipid polymorphism induced by molecular rearrangement in the headgroup region. *Biophys. J.* 73:870–877.

Hübner, W., and H. H. Mantsch. 1991. Orientation of specifically $^{13}C{=}O$ labeled phosphatidylcholine multilayers from polarized attenuated total reflection FT-IR spectroscopy. *Biophys. J.* 59:1261–1272.

Hupfer, B., H. Ringsdorf, and H. Schupp. 1983. Liposomes from polymerizable phospholipids. *Chem. Phys. Lipids.* 33:355–374.

Israelachvili, J. N., and H. Wennerström. 1992. Entropic forces between amphiphilic surfaces in liquids. *J. Phys. Chem.* 96:520–531.

Juliano, R. L. and D. Layton. 1980. Drug Delivery Systems: Characteristics and Biomedical Applications. Oxford University Press, New York.

Kim, J. T., J. Mattai, and G. G. Shipley. 1987. Bilayer interactions of ether- and ester-linked phospholipids: dihexadecyl- and dipalmitoylphosphatidylcholines. *Biochemistry.* 26:6592–6598.

Kint, S., P. H. Wermer, and J. R. Scherer. 1992. Raman spectra of hydrated phospholipid bilayers. 2. Water and head-group interactions. *J. Phys. Chem.* 96:446–452.

Klose, G., K. Arnold, G. Peinel, H. Binder, and K. Gawrisch. 1985. The structure and dynamics of water near membrane surfaces. *Colloids Surfaces.* 14:21–30.

Koenig, B. W., H. H. Strey, and K. Gawrisch. 1997. Membrane lateral compressibility measured by NMR and x-ray diffraction—effect of acyl chain polyunsaturation. *Biophys. J.* 73:1954–1966.

Kornyshev, A. A., and S. Leikin. 1989. Fluctuation theory of hydration forces: the dramatic effect of inhomogeneous boundary conditions. *Phys. Rev. A.* 40:6431–6437.

Lee, Y.-S., J.-Z. Yang, T. M. Sisson, D. A. Frankel, J. T. Gleeson, E. Aksay, S. L. Keller, S. M. Gruner and D. F. O'Brien. 1995. Polymerization of nonlamellar lipid assemblies. *J. Am. Chem. Soc.* 117: 5573–5578.

Leikin, S., V. A. Parsegian, D. C. Rau. 1993. Hydration forces. *Annu. Rev. Phys. Chem.* 44:369–395.

Lewis, R. N. A. H., W. Pohle, and R. N. McElhaney. 1996. The interfacial structure of phospholipid bilayers: differential scanning calorimetry and Fourier transform infrared spectroscopic studies of 1,2-dipalmitoyl-sn-glycero-3-phosphorylcholine and ist dialkyl and acyl-alkyl analogs. *Biophys. J.* 70:2736–2746.

Li, P. C., and J. P. Devlin. 1973. Glassy water Raman spectrum from a trapped laser beam. *J. Chem. Phys.* 59:547–548.

Luzzati, V. 1968. X-ray diffraction studies of lipid-water systems. *In* Biological Membranes, Vol. 1. D. Chapman, editor. Academic Press, London. 71–123.

Marcelja, S., and N. Radic. 1976. Repulsion of interfaces due to boundary water. *Chem. Phys. Lett.* 42:129–130.

Marsh, D. 1990. Handbook of Lipid Bilayers. CRC Press, Boca Raton, FL.

McGraw, R., W. G. Madden, M. S. Bergren, S. A. Rice, and M. G. Sceats. 1978. A theoretical study of the OH-stretching region of the vibrational spectrum of ice Ih. *J. Chem. Phys.* 69:3483–3495.

McIntosh, T. J. 1980. Differences in hydrocarbon chain tilt between hydrated phosphatidylethanolamine and phosphatidylcholine bilayers. A molecular packing model. *Biophys. J.* 29:237–246.

McIntosh, T. J., A. D. Magid, and S. A. Simon. 1987. Steric repulsion between phosphatidylcholine bilayers. *Biochemistry.* 26:7325–7332.

McIntosh, T. J., and S. A. Simon. 1986. Hydration force and bilayer deformation: a reevaluation. *Biochemistry.* 25:4058–4066.

McIntosh, T. J., and S. A. Simon. 1993. Contributions of hydration and steric (entropic) pressures to the interactions between phosphatidylcholine bilayers: experiments with the subgel phase. *Biochemistry.* 32: 8374–8384.

Ohno, H., Y. Ogata, and E. Tsuchida. 1987. Polymerization of liposomes composed of diene-containing lipids by UV and radical initiators: evidence for the different chemical environment of diene groups on 1- and 2-acyl chains. *Macromolecules.* 20:929–933.

Okamura, E., J. Umemura, and T. Takenaka. 1990. Orientation studies of hydrated dipalmitoylphosphatidylcholine multibilayers by polarized FT-IR ATR spectroscopy. *Biochim. Biophys. Acta.* 1025:94–98.

O'Leary, T. J., and J. T. Mason. 1996. A new phase in phosphatidylcholines. *Biophys. J.* 71:2915–2916.

Parsegian, V. A., N. Fuller, and R. P. Rand. 1979. Measured work of deformation and repulsion of lecithin bilayers. *Proc. Natl. Acad. Sci. USA.* 76:2750–2754.

Pascher, I., M. Lundmark, P.-G. Nyholm, and S. Sundell. 1992. Crystal structures of membrane lipids. *Biochim. Biophys. Acta.* 1113:339–373.

Pearson, R. H., and I. Pascher. 1979. The molecular structure of lecithin dihydrate. *Nature.* 281:499–501.

Peinel, G., H. Frischleder, and H. Binder. 1983. Quantum-chemical and empirical calculations on phospholipids. VIII. The electrostatic potential from isolated molecules up to layer systems. *Chem. Phys. Lipids.* 33: 113–123.

Rand, P. 1981. Interacting phospholipid bilayers: measured forces and induced structural changes. *Annu. Rev. Biophys. Bioeng.* 10:277–314.

Rand, R. P., and V. A. Parsegian. 1989. Hydration forces between phospholipid bilayers. *Biochim. Biophys. Acta.* 988:351–376.

Ruocco, M. J., D. J. Siminovich, and R. H. Griffin. 1985. Comparative study of the gel phases of ether- and ester-linked phosphatidylcholines. *Biochemistry.* 24:2406–2411.

Sceats, M. G., M. Stavola, and S. A. Rice. 1979. On the role of Fermi resonance in the spectrum of water in the condensed phases. *J. Chem. Phys.* 71:983–990.

Scherer, J. R. 1989. On the position of the hydrophobic/hydrophilic boundary in lipid bilayers. *Biophys. J.* 55:957–964.

Snyder, R. G., G. L. Liang, H. L. Strauss, and R. Mendelsohn. 1996. IR spectroscopic study of the structure and phase behavior of long-chain diacylphosphatidylcholines in the gel state. *Biophys. J.* 71:3186–3198.

Straume, M., and B. J. Litman. 1987. Equilibrium and dynamic structure of large, unilamellar, unsaturated acyl chain phosphatidylcholine vesicles as determined from higher order analysis of 1,6-diphenyl-1,3,5-hexatriene and 1-[4-(trimethylammonio)phenyl-6-phenyl]-1,3,5-hexatriene anisotropy decay. *Biochemistry.* 26:5113–5120.

Sun, W.-S., S. Tristram-Nagle, R. M. Suter, and J. Nagle. 1996. Anomalous phase behavior of long chain saturated lecithin bilayers. *Biochim. Biophys. Acta.* 1279:17–24.

Tanford, C. 1973. The Hydrophobic Effect. Wiley and Sons, New York.

Tardieu, A., V. Luzzati, and F. C. Reman. 1973. Structure and polymorphism of the hydrocarbon chains of lipids: a study of lecithin-water phases. *J. Mol. Biol.* 75:711–733.

Ter-Minassian-Sara, L., E. Okamura, J. Umemura, and T. Takenaka. 1988. FT-IR ATR spectroscopy of hydration of dimyristoylphosphatidylcholine multibilayers. *Biochim. Biophys. Acta.* 946:417–423.

Ulrich, A. S., and A. Watts. 1994. Molecular response of the lipid headgroup to bilayer hydration monitored by ^{2}H-NMR. *Biophys. J.* 66: 1441–1449.

Volke, F., S. Eisenblätter, and G. Klose. 1994. Hydration force parameters of phosphatidylcholine lipid bilayers as determined from ^{2}H-NMR studies of deuterated water. *Biophys. J.* 67:1–7.

Walrafen, G. E. 1971. Raman spectral studies of the effects of solutes and pressure on water structure. *J. Chem. Phys.* 55:768–793.

Wong, P. T. T., and E. J. Whalley. 1975. Optical spectra of orientationally disordered crystals. V. Raman spectrum of ice Ih in the range 4000–350 cm^{-1}. *J. Chem. Phys.* 62:2418–2425.

Yeagle, P. L. 1978. Phospholipid Headgroup behaviour in biological assemblies. *Accounts Chem. Res.* 11:321–327.

Zhou, F., and K. Schulten. 1995. Molecular dynamics study of a membrane-water interface. *J. Phys. Chem.* 99:2194–2207.

Zundel, G. 1969. Hydration and Intermolecular Interactions. Academic Press, New York.